Multi-$\hbar\omega$ shell model analyses of elastic and inelastic proton scattering from ^{14}N and ^{16}O

S. Karataglidis, P. J. Dortmans, K. Amos, and R. de Swiniarski*
School of Physics, University of Melbourne, Parkville, Victoria, Australia, 3052
(Received 16 August 1995)

Elastic and inelastic scattering data from the scattering of 160 MeV protons from ^{14}N, and of 200 MeV protons from ^{16}O have been analyzed using a fully microscopic distorted wave approximation. The analyses involve large space (multi-$\hbar\omega$) shell model wave functions, an effective nucleon-nucleon interaction that is energy and medium dependent, and fully microscopic (nonlocal) optical potentials built with that same effective interaction. The results for ^{14}N and ^{16}O correlate with analyses of elastic and inelastic electron scattering form factors indicating that improvements are needed in the shell model interactions used to obtain the nuclear wave functions.

PACS number(s): 21.60.Cs, 25.40.Cm, 25.40.Ep, 27.20.+n

I. INTRODUCTION

Recently [1], analyses of elastic and inelastic intermediate energy proton scattering data from ^{12}C were presented in which no core polarization corrections or renormalizations were required to reproduce the magnitudes and shapes of both the differential cross sections and analyzing powers. This was achieved by using a density dependent (DD) nucleon-nucleon (NN) effective interaction, not only to specify the interaction between the probe and each and every nucleon in the target, but also, when folded with the state shell occupancies, to give the complex, nonlocal optical potentials that were used with (microscopic) shell model descriptions of the nuclear states in distorted wave approximation (DWA) calculations. The results of these calculations were correlated with those of elastic and inelastic electron scattering form factors as both studies use the same one-body density matrix elements (OBDME) obtained from multi-$\hbar\omega$ shell model wave functions. Equally good fits were obtained for those form factors, as for the proton scattering cross sections and analyzing powers.

So far only proton scattering data from ^{12}C have been analyzed using this (new) DD interaction, given the extensive data sets of many incident energies of elastic and inelastic scattering of protons. These include transitions to many positive and negative parity states in ^{12}C. There also exists a complementary set of elastic and inelastic electron scattering data exciting the same states. Also, the shell model that gave the OBDME to be used in those analyses predicted partners to every state in the experimental spectrum of ^{12}C up to an excitation energy of 20 MeV [1] and to better than 2 MeV in excitation for most states. The extensive data sets gave a quite stringent test of the DD interaction for various higher incident proton energies to 800 MeV [1,2], and favorable comparisons were found at various energies with fully microscopic DWA calculations made using the Love-Franey (LF) interaction [3,4]. From these comparisons, density effects were shown to be very important for both the elastic and inelastic scattering processes, especially for the descriptions of the analyzing powers.

The present paper reports analyses of data of elastic and inelastic proton scattering exciting states in ^{14}N and ^{16}O, at 160 and 200 MeV, respectively. For ^{16}O, the same DD interaction used to analyze the 200 MeV proton scattering data on ^{12}C is used again, while at 160 MeV the same prescription has been used to give a tabulation of the appropriate (DD) force. The DD force has now been defined, and values tabulated, for energies from 122 to 800 MeV [5]. These effective interactions have been built from mappings to g matrix elements (solutions of the Brueckner-Bethe-Goldstone equations) [6,7] and are designed for use in the DWA program, DWBA91, of Raynal [8]. The g matrix elements have been evaluated with the Paris interaction [9] as the starting potential.

The premise on which this study is undertaken is twofold. Assuming realistic wave functions describing the states involved in these scatterings, a further accurate evaluation of the DD interaction with other nuclei would result. Conversely, if the DD interaction is deemed appropriate, such analyses would test quite sensitively the wave functions obtained from the structure model, especially when they can be correlated with complementary analyses of electron scattering form factors. Both these points are addressed when analyses of both the differential cross sections and of the analyzing powers are made, as the cross sections are sensitive both to the details of the nuclear structure and to the effective interaction, while analyzing powers are especially sensitive to details of the effective interaction.

II. CALCULATION DETAILS

The shell model interaction used to obtain the states in ^{14}N and ^{16}O was that of Haxton and Johnson (HJ) [10]. This interaction consists of the Cohen and Kurath $(8-16)2$BME $0p$-shell interaction [11], the Brown and Wildenthal $1s0d$-shell interaction [12], the Millener-Kurath interaction [13] for the cross-shell elements, and the bare Kuo g matrix for the $2\hbar\omega$ interaction. It was constructed for a complete $(0+2+4)\hbar\omega$ shell model space by setting the two-body matrix elements involving all the other major shells, from the $0s$ to the $0h1f2p$ shells to zero. Thereby there is complete removal of spurious center-of-mass motion,

*On leave from the Institut des Sciences Nucléaires, IN2P3 et Université J. Fourier, 38026 Grenoble–Cedex, France.

TABLE I. States in ^{14}N and ^{16}O considered in the present study. The energies obtained from the $0\hbar\omega$, $(0+2)\hbar\omega$, and $(0+2+4)\hbar\omega$ shell models are compared to those from experiment [16,17].

Nucleus	State	Excitation energy (MeV)			
		Experiment	$0\hbar\omega$	$(0+2)\hbar\omega$	$(0+2+4)\hbar\omega$
^{14}N[a]	$1^+;0$	0.00	0.00	0.00	0.00
	$(1^+;0)$				(0.99)
	$0^+;1$	2.31	2.47	1.51	2.17
^{16}O[b]	$0^+;0$	0.00			0.00
	$0^+;0$	6.05			6.33
	$3^-;0$	6.13			8.38
	$2^+;0$	6.91			7.67
	$1^-;0$	7.12			9.12

[a]Experimental values from Ref. [16].
[b]Experimental values from Ref. [17].

and, by not permitting radial one-particle–one-hole (1p-1h) $2\hbar\omega$ single-particle excitations, the Hartree-Fock condition is satisfied. The Hamiltonian then was diagonalized in a $(0+2+4)\hbar\omega$ space, for the positive parity states of ^{14}N and ^{16}O, using the Dubach-Haxton version of the GLASGOW shell model code [14]. The negative parity states of ^{16}O were obtained in a restricted $(1+3+5)\hbar\omega$ space, where the restriction was the exclusion of single-particle transitions from the $0p$ up to the $0i1g2d3s$ shell. This restriction did not create any serious problem with spuriosity (due to center-of-mass motion) in the wave functions of the states of interest listed in Table I. All center-of-mass energy eigenvalues for those (positive and negative parity) states in ^{16}O were 19.19 MeV, indicating that such spuriosity was completely removed as well for the negative parity states in the calculated spectrum. In the case of ^{14}N, a complete $(0+2)\hbar\omega$ calculation was also performed using the MK3W interaction [1,15] and the OXBASH program [15]. As well, $0\hbar\omega$ shell model wave functions were calculated using the Cohen and Kurath $(8-16)$2BME interaction [11].

While the results of the $(0+2+4)\hbar\omega$ shell model calculation accurately reproduce the low-lying states of ^{14}N and ^{16}O (the HJ interaction was designed to do so for ^{16}O [10]), a state is predicted in ^{14}N at 0.99 MeV excitation for which the corresponding observed state is at 6.20 MeV [16]. The wave function for this state is

$$|0.99\ \text{MeV}\rangle = 25.10\%|0\hbar\omega\rangle + 64.77\%|2\hbar\omega\rangle + 10.13\%|4\hbar\omega\rangle.$$

Such a highly deformed state at this low excitation energy cannot be considered realistic, and may be due to the choice of the $2\hbar\omega$ interaction and/or to the fact that the specific (shell model) interactions we have used in the extended model space calculation were optimized for use in calculations with much smaller bases.

The isoscalar excitation of the $1_1^-;0$ (7.12 MeV) state in ^{16}O, from the ground state, is particularly interesting as it relates to the expectation value for the position of the center of mass, which must tend to zero [18]. The value of the constraint integral for such a transition [Eqs. (15) and (16) of Ref. [1]], using the OBDME obtained from the $(0+2+4)\hbar\omega$ shell model calculation, was 0.058 fm.

We have used the nuclear structure results in analyses of elastic and inelastic electron scattering form factors and in analyses of proton elastic and inelastic scattering data (cross sections and analyzing powers). The analyses of such complementary data, electron scattering form factors, and proton cross sections, etc., provide stringent tests of the spectroscopic model wave functions, but only when a fully microscopic theory of proton scattering from nuclei (in a DWA for inelastic scattering) is used. A fully microscopic prescription of elastic and inelastic proton scattering is implemented in coordinate space by the program DWBA91, and the theoretical development of that model, including discussion of the effective interaction, is given in Refs. [1,6,7]. Sufficient details are given again herein to specify those elements which are important in the description of the nucleon-nucleus (NA) scattering process. Specifically, the attributes of the many-fermion nuclear structure required in analyses are the shell occupancies for each state as well as the OBDME for each inelastic transition. The single-particle (bound state) wave functions are also needed as is a density profile of the nucleus to specify the DD interaction for each point in the nuclear medium.

The nuclear wave functions were obtained from the shell model calculations described previously, from which the OBDME,

$$S_{j_1 j_2 I} = \langle J_f \| [a_{j_2}^\dagger \times \tilde{a}_{j_1}]^I \| J_i \rangle, \tag{1}$$

are a result. The OBDME are the weights for each allowed single-particle transition matrix element in which the particle from orbital j_1 is excited to orbital j_2, with an angular momentum transfer of I. Also, the nuclear wave functions provide the shell occupancies required to specify the complex, fully nonlocal, microscopic optical potentials, involved in these DWA calculations. For the elastic scattering process, the OBDME reduce to the shell occupancies. These shell occupancies and OBDME for the inelastic transitions considered herein have been tabulated [19].

Often in DWA calculations, the single-particle bound state wave functions are specified as harmonic oscillator wave functions. It is more appropriate, though, to use Woods-Saxon bound state wave functions determined by analysis of the elastic electron scattering form factor [1]. The latter are eigenfunctions of the single-particle Hamiltonian in which

TABLE II. Density profile defining the DD (NN) effective interaction for ^{12}C, ^{14}N (at 160 MeV) and ^{16}O (at 200 MeV) [32]. The kinematic factor to convert to the NA interaction is also given.

Nucleus	ρ_0 (nucleons/fm^3)	c (fm)	z (fm)	w	Kinematic factor
^{12}C	0.182	2.355	0.522	−0.149	0.94792
^{14}N	0.179	2.570	0.505	−0.180	0.94536
^{16}O	0.165	2.608	0.513	−0.051	0.89430

$$V=V_0\left[1+2\lambda[l\cdot s]\left(\frac{\hbar}{m_\pi c}\right)^2\frac{1}{r}\frac{d}{dr}\right]f(r,R,a), \tag{2}$$

where, with $R=r_0A^{1/3}$,

$$f(r,R,a)=\left[1+\exp\left(\frac{r-R}{a}\right)\right]^{-1}. \tag{3}$$

The values appropriate for ^{12}C are listed in Table II of Ref. [1]. Those we have used for ^{14}N are identical, except for simplicity we have set $\lambda=0$.

The density profile assumed for the DD interaction is the three-parameter Fermi distribution [1]

$$\rho(r)=\frac{\rho_0(1+wr^2/c^2)}{1+e^{(r-c)/z}}, \tag{4}$$

for which the parameter values appropriate for ^{12}C, ^{14}N, and ^{16}O are listed in Table II. The kinematic correction required to convert the effective NN interaction to an effective NA interaction, as given by Eq. (19) of Ref. [3], is also listed therein.

III. ANALYSES OF ELECTRON SCATTERING FORM FACTORS

Herein we report on analyses of the elastic electron scattering form factors for ^{14}N and ^{16}O. The one-body charge operator of deForest and Walecka [20] was used in calculations of the electron scattering longitudinal form factors. The calculated form factors also included corrections for recoil and the single-nucleon form factor. The inelastic longitudinal electron scattering form factor for the $0^+\rightarrow 1^-_1;0$ (7.12 MeV) transition in ^{16}O was also studied as complementary to the inelastic proton scattering data. The other transition of special interest is the magnetic dipole excitation of the $0^+;1$ (2.313 MeV) state in ^{14}N. The electron scattering form factor for this magnetic dipole transition we expect to be strongly affected by meson exchange currents (MEC). The associated amplitudes of those MEC involve the two-body density matrix elements of structure; values that are unavailable to us at present. Thus we report only the analyses of proton inelastic scattering to this state since hadronic excitation is not so influenced by the MEC.

The longitudinal elastic scattering form factor for ^{14}N is displayed in Fig. 1, wherein the data of Dally *et al.* [21] are compared to the results of the calculations of the $C0$ longitudinal form factor. There is excellent agreement with the data when using both the harmonic oscillator (solid curve) and Woods-Saxon (dashed curve) single-particle wave functions, indicating that either of these sets are suitable for use in analyses of inelastic scattering data. The harmonic oscillator length used was 1.64 fm.

The elastic scattering form factor for ^{16}O is displayed in Fig. 2, wherein the data of Sick and McCarthy [22] are compared to the results of the calculation made using the ground state shell occupancies from the $(0+2+4)\hbar\omega$ shell model calculation. Harmonic oscillator single-particle wave functions were used in this calculation and the oscillator length was 1.7 fm. The calculated result reproduces the data reasonably well, except for the third maximum ($q>3$ fm^{-1}). However, in this region of high momentum transfer, a modification in the one-body charge density is required to fit the data [22]. Construction of an orthogonal set of bound state

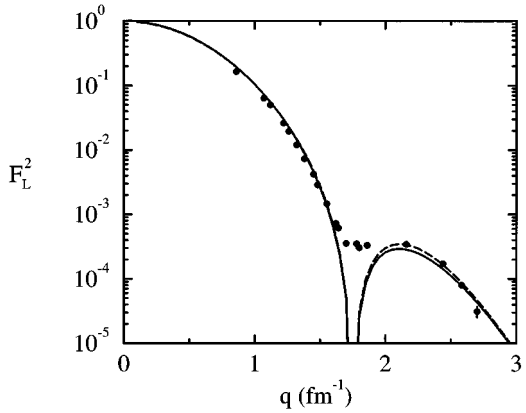

FIG. 1. Longitudinal elastic electron scattering form factor for ^{14}N. The data of Dally *et al.* [21] are compared to the results of the calculations of the $C0$ form factor using harmonic oscillator (solid line) and Woods-Saxon (dashed line) single-particle wave functions.

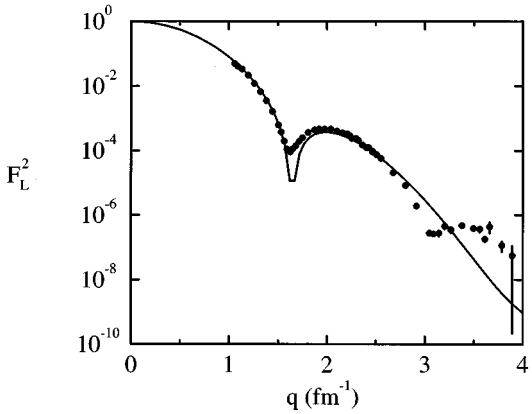

FIG. 2. Elastic electron scattering form factor for ^{16}O. The data of Sick and McCarthy [22] are compared to the result found using the $(0+2+4)\hbar\omega$ shell model structure and with harmonic oscillator single-particle wave functions.

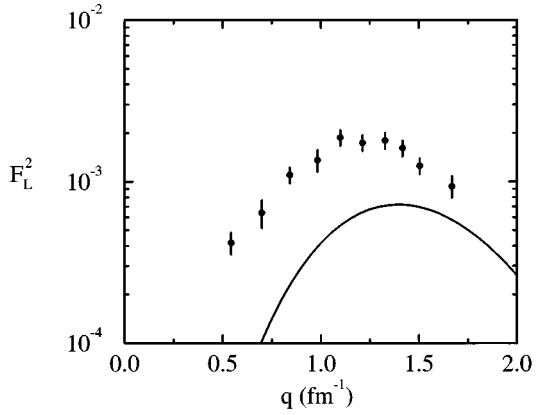

FIG. 3. Longitudinal form factor for the $0^+ \rightarrow 1_1^-;0$ (7.12 MeV) transition in ^{16}O. The data of Torizuka *et al.* [23] are compared to the results of the $(1+3+5)\hbar\omega$ calculation.

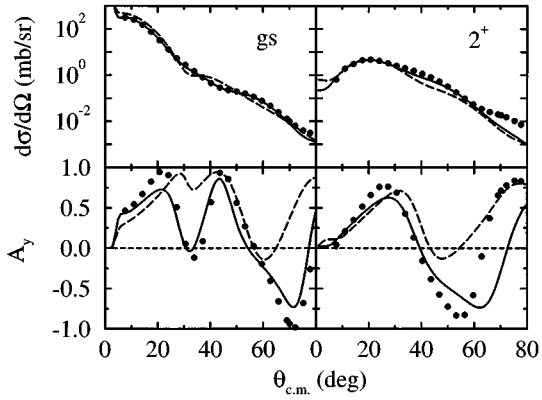

FIG. 4. Differential cross sections and analyzing powers for the elastic scattering (labeled gs) and inelastic scattering (labeled 2^+), exciting the $2^+;0$ (4.44 MeV) state, of 160 MeV protons from ^{12}C. The elastic scattering data of Meyer *et al.* [27] and inelastic scattering data of Hugi *et al.* [29] are compared to the results of the calculations made using the DD (solid line) and LF (dashed line) forces.

Woods-Saxon wave functions is difficult given the size of the single-particle basis spanned by the chosen shell model space.

The longitudinal electron scattering form factor for the $0^+ \rightarrow 1_1^-;0$ (7.12 MeV) transition in ^{16}O is displayed in Fig. 3. Herein, the data of Torizuka *et al.* [23] are compared to the result of the calculation we have made using the $(1+3+5)\hbar\omega$ shell model wave functions. The result underestimates the data by a factor of 2.6, and places the peak at 1.4 fm^{-1}; a value larger than that indicated by the data. The disagreement could be due to the neglect of the 1p-1h $3\hbar\omega$ and $5\hbar\omega$ matrix elements in the shell model interaction and which may be necessary to describe this negative parity transition. While there is evidence of weak isospin mixing ($\sim$1%) in this $1^-;0$ state, as evidenced by the observed nonzero $B(E1)$ value for the ground state decay [18], the dominant $T=0$ character of the state overwhelms the $T=1$ component in the electron scattering form factor with increasing q [18], suggesting that isospin mixing does not affect these form factors. In a previous calculation of the longitudinal electron scattering form factor [18], using OBDME satisfying the constraint associated with isoscalar electric dipole transitions [Eq. (15) of Ref. [1]] and as obtained from the $1\hbar\omega$ wave functions of Millener and Kurath [13], core polarization corrections were sufficient (and necessary) to obtain agreement with data.

IV. ANALYSES OF ELASTIC AND INELASTIC PROTON SCATTERING DATA

The differential cross section and analyzing power data for the elastic and inelastic scattering of 160 MeV protons from ^{14}N have been analyzed, as have the data for the elastic and inelastic scattering of 200 MeV protons from ^{16}O. But we first report on an analysis of 160 MeV proton scattering from ^{12}C as a control upon the effective (DD) interaction required in the other analyses.

The data for the differential cross sections and analyzing powers for elastic scattering of protons from ^{12}C, for energies from 200 to 800 MeV have been analysed previously using the DD interaction [1,2], where the importance of density effects was demonstrated. The inelastic scattering of protons in the same energy range was also studied [1,2] using the DWA with OBDME obtained from the $(0+2)\hbar\omega$ and $(1+3)\hbar\omega$ model spectroscopies [19], for the positive and negative parity states, respectively. For those inelastic scattering transitions, density effects were again important, and the techniques developed allowed conjecture about the (hitherto ambiguous) spin-isospin assignments of several negative parity states [24].

We stress that we analyse the scattering data using a fully microscopic theory. Both the elastic scattering optical model potentials and the inelastic scattering amplitudes (in the DWA) are evaluated using an effective NN interaction that has been developed from an accurate mapping of the NN g matrices of the Paris potential for diverse infinite nuclear matter densities [7]. The optical model potentials that result from folding the effective interaction with the target density matrix elements are nonlocal and the associated nonlocal Schrödinger equations have been solved to give the scattering phase shifts from which the elastic scattering cross section and analyzing powers have been calculated. They have been used also to specify the distorted waves required in DWA calculations of the inelastic scattering quantities. The inelastic scattering amplitudes arising from a fully antisymmetrized theory predicated upon the same effective NN g matrices used to specify the nonlocal optical potentials. Therefore higher-order (many-body) corrections to the NA G matrices, such as the Cheon rearrangement terms in the inelastic amplitudes [25], are not included. Such terms have been applied in studies involving local density approximations leading to local interactions [25,26], but it is not clear what form these many-body corrections would take in analyses that include both direct and exchange diagrams in both the elastic and inelastic channels.

In our studies we have compared the results so found using the new (DD) effective interaction with those obtained using the LF interactions [3,4] which are based upon a fit to the free NN scattering amplitudes by a sum of Yukawa terms.

In Fig. 4 the cross sections and analyzing powers from the scattering of 160 MeV protons from ^{12}C, both elastically and inelastically to the $2^+;0$ (4.44 MeV) state are displayed.

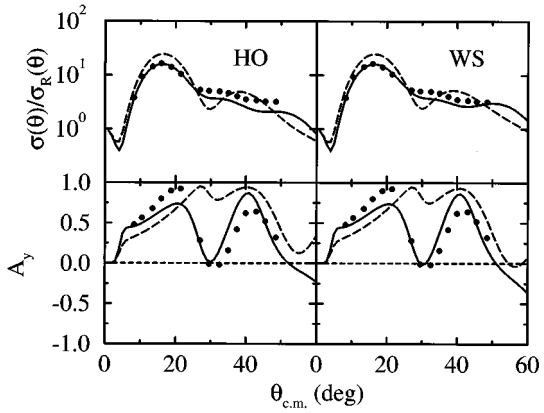

FIG. 5. Differential cross section and analyzing power for the elastic scattering of 160 MeV protons from ^{14}N. The results in the left-hand panel (HO) were obtained using harmonic oscillator wave functions, while those in the right-hand panel (WS) were obtained using Woods-Saxon wave functions. The data of Taddeucci *et al.* [30] are compared to the results obtained using the DD (solid line) and LF (dashed line) forces.

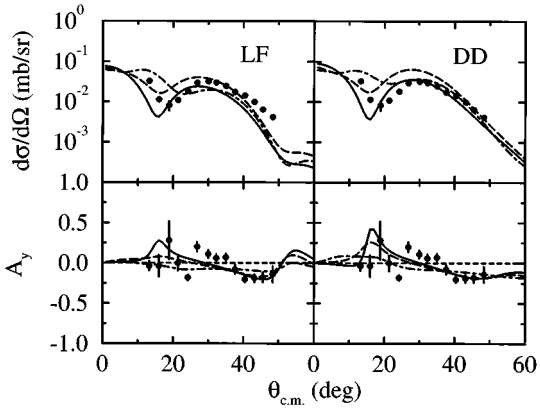

FIG. 6. Differential cross section and analyzing power for the inelastic scattering of 160 MeV protons from ^{14}N, exciting the $0^+;1$ (2.313 MeV) state. The data of Taddeucci *et al.* [30] are compared to the results obtained using the $(0+2+4)\hbar\omega$, $0\hbar\omega$, and $(0+2)\hbar\omega$ spectroscopies and given by the solid, dashed, and dot-dashed lines, respectively. The effective interactions used in the calculations are as indicated.

Therein, the data of Meyer *et al.* [27] to 80° in the center of mass [28] are compared to the results of our fully microscopic model calculations that were made using the DD interaction (solid line) and the LF interaction (dashed line). The elastic and inelastic data are displayed in the left-hand (gs) and right-hand (2^+) panels, respectively. The OBDME were obtained from the $(0+2)\hbar\omega$ shell model calculation described in Refs. [1,19]. While both the DD and LF results for the elastic scattering cross section are in general agreement with the chosen data, the result using the DD force is the better one. The density effects are illustrated far more clearly in the results for the analyzing power, where the DD result is a significant improvement over that obtained using the LF force. This is typically the case when density effects are introduced. The same effects are demonstrated in the results for the scattering to the $2^+;0$ (4.44 MeV) state, where the data of Hugi *et al.* [29], again just to 80° in the center of mass [28], are compared to the results of our calculations. The result obtained using the DD force agrees with the data to 60°, while the LF result fails to reproduce the data beyond 30°. Again, the differences, due to the inclusion of density effects, are more pronounced in the results for the analyzing power, with the DD result being in far better agreement with the data. Thus we are confident that the DD interactions at 160 and 200 MeV are appropriate for use in analyses of scattering data from ^{14}N and ^{16}O.

In Fig. 5 we compare the results of our calculations of the elastic scattering of 160 MeV protons from ^{14}N with the data of Taddeucci *et al.* [30]. Herein the ratio to the Rutherford cross section data are compared to the results of the calculations made using the DD force (solid line) and the LF force (dashed line). The results in the left-hand panel (HO) used harmonic oscillator wave functions, while those in the right-hand panel (WS) used those of Woods-Saxon form. With either choice of single-particle wave functions, the DD cross-section result better reproduces the shape of the data and the result found using the Woods-Saxon wave functions is slightly better so far as the magnitude is concerned, particularly at large scattering angles. As for ^{12}C, the g matrix density effects are dramatically illustrated in the results for the analyzing power. The calculations made using the LF force do not match the observed minimum in the data at 30°, but the DD result does so very well. All three models of structure give essentially the same results.

The differences between the three models of structure $[0\hbar\omega, (0+2)\hbar\omega$, and $(0+2+4)\hbar\omega]$ are realized clearly in the results for the cross section and analyzing power for the inelastic scattering of 160 MeV protons to the $0^+;1$ (2.313 MeV) state in ^{14}N. The results of the three model calculations are compared to the data of Taddeucci *et al.* [30] in Fig. 6. Therein, the results of the $(0+2+4)\hbar\omega$ calculation are displayed by the solid line while those of the $0\hbar\omega$ and $(0+2)\hbar\omega$ calculations are displayed by the dashed and dot-dashed lines, respectively. Best agreement with the cross-section data, and particularly above the minimum at 20°, is achieved using the $(0+2+4)\hbar\omega$ spectroscopy. The effect of increasing the shell model space from $0\hbar\omega$ to $(0+2+4)\hbar\omega$ is to reduce the magnitude of the predicted cross section to be in better agreement with the data. The DD result obtained using the $(0+2+4)\hbar\omega$ spectroscopy does best of all, giving a better representation of the shape of the cross section at large angles when compared to the equivalent LF result. The results using the $(0+2)\hbar\omega$ shell model OBDME are particularly poor. This cross section has a peak near 12°, which is not observed in the data, and the position of the minimum is moved then beyond 20°. The analyzing power data suggest that there is a peak at 20°. Such is only reproduced by both $(0+2+4)\hbar\omega$ calculations, as well the $0\hbar\omega$ calculation made using the DD force. This feature is more pronounced in the results using the DD force. The analyzing power results for the other model spectroscopies are very small and unstructured. We surmise that the $(0+2)\hbar\omega$ shell model calculation obtained using the MK3W interaction [1,15] does not give realistic wave functions for ^{14}N, indicating the need for inclusion of $4\hbar\omega$ components in the wave functions of ^{14}N.

The results of the elastic scattering (labeled gs) and of select inelastic scatterings of 200 MeV protons from ^{16}O are

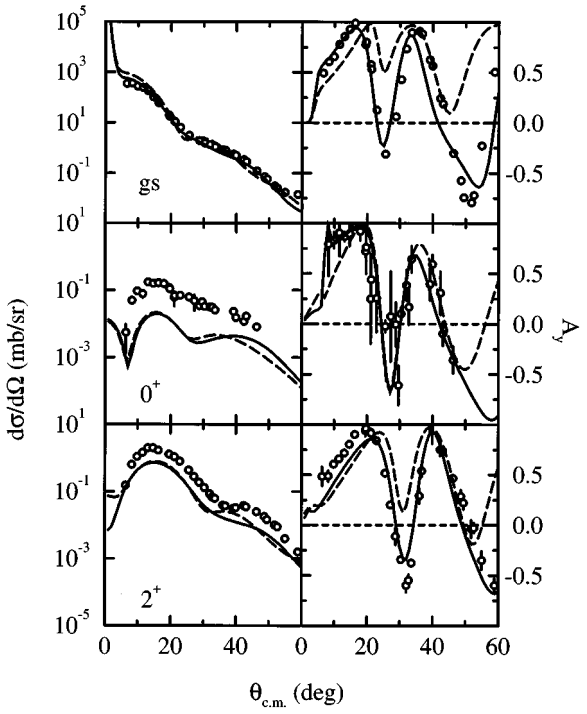

FIG. 7. Differential cross section and analyzing power for the elastic scattering and inelastic scattering of 200 MeV protons from ^{16}O. The elastic scattering results are displayed in the top panel (gs), while the inelastic scattering results to the $0_2^+;0$ (6.05 MeV) and $2_1^+;0$ (6.91 MeV) states are in the middle and bottom panels, respectively. The data of Seifert *et al.* [31] are compared to the results of the DD calculation (solid line) and the LF calculation (dashed line).

shown in Fig. 7. The excitations of the $0_2^+;0$ (6.05 MeV) and $2_1^+;0$ (6.91 MeV) states (labeled by 0^+ and 2^+, respectively) are shown specifically. Herein, the data of Seifert *et al.* [31] are compared to the results of the calculations made using the $(0+2+4)\hbar\omega$ spectroscopy with the DD force (solid lines) and with the LF force (dashed lines). The elastic scattering cross-section data are well reproduced by both the DD and LF calculations, with slightly better agreement between the DD results and the data, reflecting the importance of g matrix medium effects. That is more clearly illustrated in the analyzing power results. The result of the DD calculation shown therein reproduces all the features of the data and is in far better agreement with them than is the LF result.

Both the DD and the LF calculations reproduce the shape of the inelastic scattering data to the $0_2^+;0$ (6.05 MeV) state. However, both calculations underestimate the observed magnitude by a factor of 10. As the cross section is weak, any small changes in the OBDME for this weak transition may result in large changes to the calculated magnitudes. With the analyzing power, however, the result of the calculation made using the DD force reproduces the shape and magnitude of the data, while the LF calculation does not match the data at small scattering angles. There is clearly a deficiency in the specification of the spectroscopy. Specifically, the HJ interaction, in setting to zero all the matrix elements involving the orbits outside of the $0p1s0d$ shells, has lost strength in this

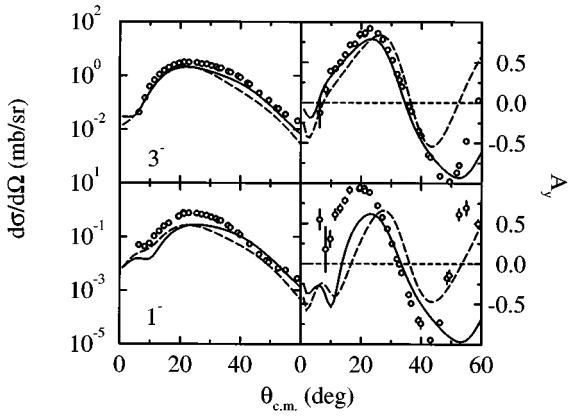

FIG. 8. As for Fig. 7, but for the inelastic scattering to the $3_1^-;0$ (6.13 MeV) and $1_1^-;0$ (7.12 MeV) states, labeled by 3^- and 1^-, respectively.

transition coming from interactions involving these other orbits.

This problem is reflected also in the results for the inelastic scattering to the $2_1^+;0$ (6.91 MeV) state that are displayed in Fig. 7, but to a lesser extent. For this transition, both the DD and LF force calculations underestimate the magnitude of the cross section by a factor of 2.5. Allowing this scaling, the result of the DD calculation is better in reproducing the shape of the data. This is also the case in the analyzing power, in which the DD result alone reproduces the observed large negative values at 30° and 60°.

In Fig. 8, the results of DWA calculations of the inelastic scattering of 200 MeV protons to the $3_1^-;0$ (6.13 MeV) and $1_1^-;0$ (7.12 MeV) states in ^{16}O are shown. These transitions are identified by the labels 3^- and 1^-, respectively. The identification of the results of the calculations are as for Fig. 7. The results for the scattering to the $3_1^-;0$ state best reproduce the magnitude of any of the inelastic cross sections from ^{16}O investigated in this study. An enhancement of 50% brings the calculations into excellent agreement with the data. Of the calculations, those made using the DD force give results that better reproduce the shape of the cross-section and analyzing power data. However, neither calculation (DD or LF) is able to match the cross-section data for the scattering to the $1_1^-;0$ (7.12 MeV) state. The differences (compared with the data) in shape and magnitude of the cross sections found with both calculations are consistent with the results found for the longitudinal inelastic electron scattering form factor (Fig. 3).

V. CONCLUSIONS

Analyses of elastic and inelastic proton scattering data from ^{12}C, ^{14}N, and ^{16}O have been made using two classes of effective NN interactions within a fully microscopic theory of elastic and (DWA) inelastic scattering. The first of these was a set of energy and density-dependent forces based on the Paris NN interaction and the second was the set of forces of Love and Franey. In the scattering analyses, $0\hbar\omega$ and multi-$\hbar\omega$ shell model descriptions of the nuclei have been used to obtain the relevant structure information

(OBDME). The results obtained for the elastic scattering cross sections and analyzing powers for ^{12}C, ^{14}N, and ^{16}O highlight the importance of density effects in the description of the *NA* scattering process. When considered with the results previously published for ^{12}C, the present ones confirm the applicability of the specified DD force (at 160 and 200 MeV) for a number of *p*-shell nuclei. In the case of the inelastic scattering of protons from ^{14}N and ^{16}O, the results for the analyzing powers also confirm the importance of *g* matrix density effects in analyses of scattering data and demonstrate further the applicability of the DD force in the description of inelastic *NA* scattering processes.

Given the propriety of the effective *NN* interactions our other results indicate a problem with the nuclear structure models. The results of the calculations are not perfectly matched with the cross-section data. Of the three models of structure used, the $(0+2+4)\hbar\omega$ model is the best for use in a description of the 160 MeV proton scattering to the $0^+;1$ (2.313 MeV) state in ^{14}N. Even so, the data suggest that a more complete description of the nuclear states is required, as none of the model wave functions considered for that process when used in DWA calculations give results that have the correct behavior at low momentum transfer. This is more evident for the inelastic scattering of 200 MeV protons from ^{16}O. Therein, while the shapes of the cross sections for all but the $1^-;0$ state are consistent with observations, all calculated DWA magnitudes must be enhanced to match data. Such core polarization reflects limitations with the chosen spectroscopy and in this case a first need is for a shell model interaction that accounts for all possible interactions between all of the particles in the active orbits.

ACKNOWLEDGMENTS

The authors wish to thank Professor Wick Haxton for his assistance in running the Dubach-Haxton version of the GLASGOW shell model code. One of us (S.K.) would like to thank the Institute for Nuclear Theory, University of Washington for its support and hospitality. The financial support of the Australian Research Council (ARC) is gratefully acknowledged as is the hospitality of the staff and students of the School of Physics in the University of Melbourne shown to R.deS. during a visit sponsored in part by the ARC and during which much of this work was done.

[1] S. Karataglidis, P. J. Dortmans, K. Amos, and R. de Swiniarski, Phys. Rev. C **52**, 861 (1995).
[2] P. J. Dortmans, S. Karataglidis, K. Amos, and R. de Swiniarski, Phys. Rev. C **52**, 3224 (1995).
[3] W. G. Love and M. A. Franey, Phys. Rev. C **24**, 1073 (1981).
[4] M. A. Franey and W. G. Love, Phys. Rev. C **31**, 488 (1985).
[5] P. J. Dortmans and K. Amos, University of Melbourne Report No. UM-P-95/41, 1995 (unpublished).
[6] H. V. von Geramb, K. Amos, L. Berge, S. Bräutigam, H. Kohlhoff, and A. Ingermarsson, Phys. Rev. C **44**, 73 (1991).
[7] P. J. Dortmans and K. Amos, Phys. Rev. C **49**, 1309 (1994).
[8] J. Raynal, computer program DWBA (NEA 1209/02).
[9] M. Lacombe, B. Loiseau, J. M. Richard, R. Vinh Mau, J. Côté, P. Pirès, and R. de Tourreil, Phys. Rev. C **21**, 861 (1980).
[10] W. C. Haxton and C. Johnson, Phys. Rev. Lett. **65**, 1325 (1990).
[11] S. Cohen and D. Kurath, Nucl. Phys. **73**, 1 (1965).
[12] B. A. Brown and B. H. Wildenthal, Annu. Rev. Nucl. Part. Sci. **36**, 29 (1988).
[13] D. J. Millener and D. Kurath, Nucl. Phys. **A255**, 315 (1975).
[14] W. C. Haxton, *Dubach-Haxton version of the* GLASGOW *program*, private communication; R. R. Whitehead, A. Watt, B. J. Cole, and I. Morrison, Adv. Nucl. Phys. **9**, 123 (1977).
[15] A. Etchegoyen, W. D. M. Rae, and N. S. Godwin, OXBASH-MSU (the Oxford–Buenos-Aries–Michigan State University shell model code) (MSU version by B. A. Brown, 1986); B. A. Brown, A. Etchegoyen, and W. D. M. Rae, MSUCL Report No. 524, 1986 (unpublished).
[16] F. Ajzenberg-Selove, Nucl. Phys. **A523**, 1 (1991).
[17] D. R. Tilley, H. R. Weller, and C. M. Cheves, Nucl. Phys. **A564**, 1 (1993).
[18] K. Amos, R. de Swiniarski, and L. Berge, Nucl. Phys. **A485**, 493 (1988).
[19] S. Karataglidis, University of Melbourne Report No. UM-P-95/43, 1995 (unpublished); University of Melbourne Report No. UM-P-95/29, 1995 (unpublished).
[20] T. deForest and J. D. Walecka, Adv. Phys. **15**, 1 (1966).
[21] E. B. Dally, M. G. Croissiaux, and B. Schweitz, Phys. Rev. C **2**, 2057 (1970).
[22] I. Sick and J. S. McCarthy, Nucl. Phys. **A150**, 631 (1970).
[23] Y. Torizuka *et al.*, Phys. Rev. Lett. **22**, 544 (1969).
[24] S. Karataglidis, P. J. Dortmans, K. Amos, and R. de Swiniarski, Aust. J. Phys. (in press).
[25] T. Cheon, K. Takayanagi, and K. Yazaki, Nucl. Phys. **A437**, 301 (1985).
[26] J. J. Kelly and S. J. Wallace, Phys. Rev. C **49**, 1315 (1994).
[27] H. O. Meyer, P. Schwandt, W. W. Jacobs, and J. R. Hall, Phys. Rev. C **27**, 459 (1983).
[28] Data from the scattering exist to much larger scattering angles, but are not considered (as yet) since the theoretical reaction model is not yet sufficient to predict reliably very small magnitudes in these cross sections.
[29] M. Hugi, W. Bauhoff, and H. O. Meyer, Phys. Rev. C **28**, 1 (1983).
[30] T. N. Taddeucci, J. Rapaport, C. C. Foster, and J. R. Comfort, Phys. Rev. C **28**, 969 (1983).
[31] H. Seifert *et al.*, Phys. Rev. C **47**, 1615 (1993).
[32] C. W. de Jager, H. de Vries, and C. de Vries, At. Data Nucl. Data Tables **14**, 479 (1974); H. de Vries, C. W. de Jager, and C. de Vries, *ibid.* **36**, 495 (1987).